Iterative Channel Estimation for MIMO MC-CDMA

Stephan Sand, Ronald Raulefs, and Armin Dammann
German Aerospace Center (DLR)
Oberpfaffenhofen, 82234 Wessling, Germany
Email: stephan.sand@dlr.de

Abstract

In this paper, we investigate the performance of a downlink multiple-input multiple-output (MIMO) multi-carrier code division multiple access (MC-CDMA) system employing a receiver with iterative channel estimation (ICE). The MC-CDMA system transmits several data symbols per user and per orthogonal frequency division multiplexing (OFDM) symbol in parallel, with each data symbol being spread with a Walsh-Hadamard code. Due to the superposition of spread data signals, (chips), zero-valued subcarriers can occur, which cannot be used to compute least-squares (LS) channel estimates in ICE. Further, the transmitted data signals coincide non-orthogonal at each receive antenna. Hence, we propose the modified LS (MLS) MIMO channel estimation method to overcome these problems and avoid noise enhancement in ICE. We further investigate the robustness of ICE with the MLS MIMO method if the channel statistics are not perfectly known.

I. INTRODUCTION

Modern wireless communication requires high data rate transmission over mobile channels. Orthogonal frequency division multiplexing (OFDM) [1] is a suitable technique for broadband transmission in multipath fading environments. For multi-carrier code division multiple access (MC-CDMA), spreading in frequency and/or time direction is introduced in addition to the coherent OFDM modulation [2]. MC-CDMA has been deemed a promising candidate for the downlink of future mobile communication systems and has recently been implemented by NTT DoCoMo in an experimental system [3]. To increase data rates further, MC-CDMA systems employ multiple-input and multiple-output (MIMO) techniques, for instance, the Alamouti space-time block code (STBC) [4].

Coherent OFDM systems require channel state information (CSI) that has to be estimated by the receiver. Therefore, pilot symbols are often periodically inserted into the transmitted signal to support channel estimation (CE). CE is performed by interpolating the time-frequency pilot grid and exploiting the correlations of the received OFDM signal [5]. These correlations are introduced by the time- and frequency-selective mobile radio channel, which is modeled as a wide-sense stationary uncorrelated scattering (WSSUS) channel [6]. The behavior of a WSSUS channel can be described by its delay and Doppler power spectral densities (PSDs). Due to the WSSUS assumption, the pilot aided channel estimation (PACE) is typically performed by cascading two one-dimensional (1-D) finite-impulse response (FIR) interpolation filters whose coefficients are based on the minimum mean square error (MMSE) criterion [5].

To further improve PACE, previously decided symbols are used as reference symbols in iterative channel estimation (ICE) [7]–[11]. In [11], the authors propose an ICE algorithm for a high mobility OFDM system based on PACE. The idea is to feed back information from the output of the channel decoder to the estimation stage. The channel decoder can significantly decrease decision feed-back errors. Additionally, it can feed back reliability information of the log-likelihood ratio values to the CE. Since the CE gets additional information from the estimated data symbols, ICE achieves a further reduction of the bit error rate (BER).

In this paper, we extend the idea of ICE to a MIMO MC-CDMA system with Walsh-Hadamard spreading codes. In [12], we propose the modified LS (MLS) channel estimation method to solve the problem of zero-valued subcarriers in ICE. When using multiple transmit antennas, the transmitted data signals coincide non-orthogonal at each receive antenna. Thus, we extend the MLS channel estimation method to cope with the non-orthogonal superposition of data symbols in ICE. We further examine the robustness of an MC-CDMA receiver with ICE and the MLS method in the downlink if the channel statistics are not known perfectly.

The paper is organized as follows. Section II introduces the downlink MIMO MC-CDMA transmission model. In Section III, PACE, ICE, the MLS method, and the extension of ICE to MIMO MC-CDMA systems are discussed. Finally, Section IV presents simulation results and Section V concludes the paper.

II. SYSTEM MODEL

Fig. 1 represents the block diagram of the downlink MIMO MC-CDMA system with ICE. At the transmitter, a binary signal of a single user out of K active users is encoded by a channel coder and interleaved by a code-bit interleaver. The bits b_k (Fig. 1(b)) are modulated and serial-to-parallel converted to M data symbols per user in an OFDM symbol. After spreading with a Walsh-Hadamard sequence of length L ($L \geq K$), the spread signals are combined, serial-to-parallel converted, and interleaved by a frequency interleaver to form the data symbol frame $S_{n,l}$ ($\{n,l\} \in \mathcal{D}$). Here, n denotes the subcarrier index, l

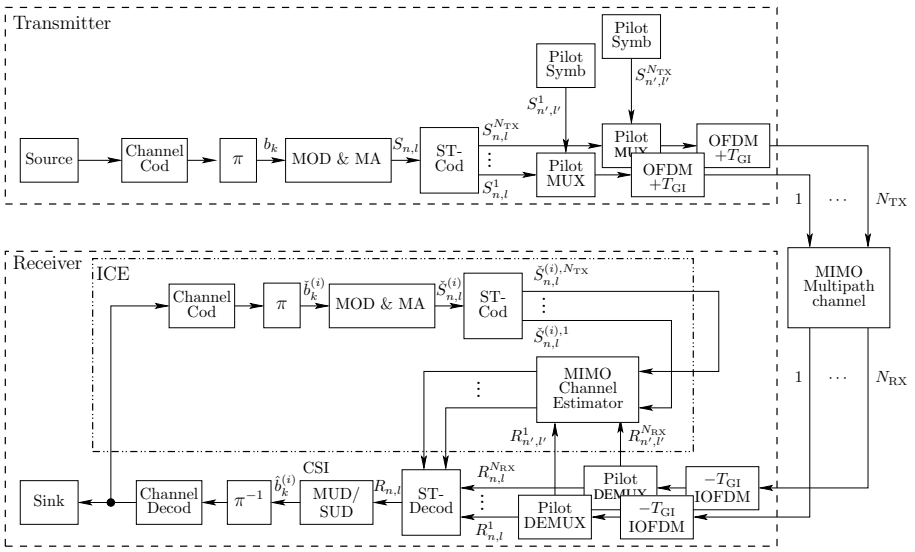

(a) MIMO MC-CDMA: transmitter and receiver with ICE

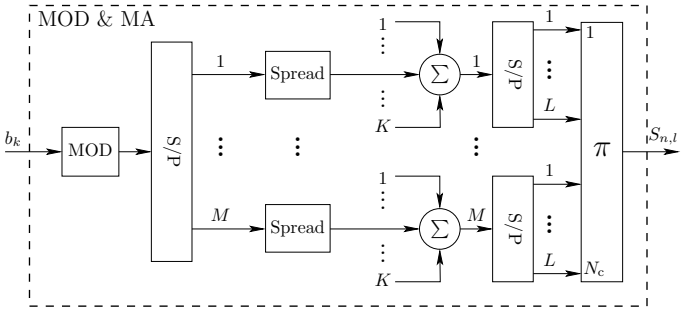

(b) Modulation and multiple access: MOD & MA

Fig. 1. Downlink MIMO MC-CDMA system with ICE

the OFDM symbol number, and $\mathcal{D}$ the set of data symbol positions in a frame. Next, $S_{n,l}$ (Fig. 1(a)) is space-time coded and each $S^m_{n,l}$ ($\{n,l\} \in \mathcal{D}^m$, $m = 1,\ldots,N_{\mathrm{TX}}$) is multiplexed together with pilot symbols $S^m_{n',l'}$, $\{n',l'\} \in \mathcal{P}^m$, $m = 1,\ldots,N_{\mathrm{TX}}$, which are inserted on a rectangular grid on disjoint positions for each transmit antenna ($\mathcal{P}^1 \cap \ldots \cap \mathcal{P}^m = \emptyset$). $\mathcal{P}^m$ denotes the set of pilot symbol positions in an OFDM frame at transmit antenna m. The set $\bar{\mathcal{D}}$ denotes the intersection of all sets $\mathcal{D}^m$ ($m = 1,\ldots,N_{\mathrm{TX}}$). In this paper, we assume that $\mathcal{D}^1 = \ldots = \mathcal{D}^m = \bar{\mathcal{D}}$. The resulting N_{TX} OFDM frames with N_{c} subcarriers and N_{s} OFDM symbols are OFDM modulated and cyclically extended by the guard interval (GI) before they are transmitted over a time-variant MIMO multipath channel, which adds white Gaussian noise.

The received symbols are shortened by the GI and OFDM demodulated for each of the N_{RX} receive antennas. Then, the received pilot symbols $R^{m,p}_{n',l'}$ ($\{n',l'\} \in \mathcal{P}^m$, $m = 1,\ldots,N_{\mathrm{TX}}$, $p = 1,\ldots,N_{\mathrm{RX}}$) are separated from the received data symbols $R^p_{n,l}$ ($\{n,l\} \in \bar{\mathcal{D}}$), and fed into the CE. In the initial ICE stage ($i = 0$), the CE only uses pilot symbols to estimate the CSI.

After demultiplexing and space-time decoding the received data symbols $R^p_{n,l}$ ($\{n,l\} \in \bar{\mathcal{D}}$), either one multi-user detector (MUD) or K single-user detector (SUD) blocks return soft-coded bits $\hat{b}^{(i)}_k$ of all users [12]. Subsequently, the bits are used to reconstruct the transmitted signal for ICE to yield the estimated transmit signal $\check{S}^{(i),m}_{n,l}$, $m = 1,\ldots,N_{\mathrm{TX}}$ (Fig. 1(a)).

In the ith iteration of ICE ($i > 0$), the CE exploits the knowledge of both the received pilot symbols $R^{m,p}_{n',l'}$ ($\{n',l'\} \in \mathcal{P}^m$) and the reconstructed transmit signal $\check{S}^{(i),m}_{n,l}$ ($\{n,l\} \in \bar{\mathcal{D}}$, $m = 1,\ldots,N_{\mathrm{TX}}$) to improve the accuracy of the CSI estimates. The newly obtained CSI estimates are fed back to the MUD/SUD block to improve the estimates of the transmitted bits. The above described ICE can be repeated to improve the performance further.

As an example for an SUD block in Fig. 1(a), consider Fig. 2. The SUD block deinterleaves the received data symbols,

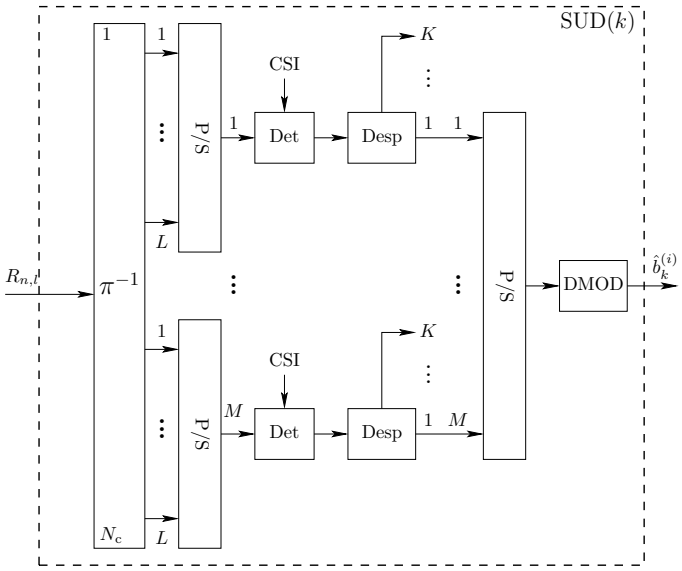

Fig. 2. Single-user detector block, user k: SUD(k)

applies a parallel-to-serial conversion for the M parallel data streams, and detects the signal of the desired user out of the K active users. We apply either a maximum ratio combiner (MRC) or an MMSE equalizer to detect the desired user signal [5]. The MRC detector will be only applied to compute the single-user bound (SUB). The detected signal is despread and soft-demodulated into soft-coded bits $\hat{b}_k^{(i)}$ by computing the log-likelihood ratio for each bit. Alternative to an SUD block in Fig. 1(a), a parallel interference canceler (PIC) can be employed as an MUD [12].

III. PILOT AIDED AND ITERATIVE CHANNEL ESTIMATION

This section investigates how PACE in the downlink can be further improved by ICE if decided data symbols are used as additional pilot symbols. Several researchers [7]–[11] have investigated ICE for spread spectrum and multi-carrier systems. However, they have not investigated ICE with a two step CE in the initial and subsequent stages for downlink MIMO MC-CDMA.

A. Pilot aided channel estimation (PACE)

Since the pilot symbols for different transmit antennas are transmitted on disjoint positions and assuming independent and identically distributed (i.i.d.) subchannels, the MIMO channel estimation reduces to estimating $N_{\mathrm{TX}} \cdot N_{\mathrm{RX}}$ SISO channels.

In the initial stage of ICE, only received pilot symbols are used to obtain the CSI in two steps [5]:

1) The initial estimate $\check{H}^{m,p}_{n',l'}$ of the channel transfer function between transmit antenna m and receive antenna p at pilot symbol positions is obtained by dividing the received pilot symbol $R^{m,p}_{n',l'}$ by the originally transmitted pilot symbol $S^{m}_{n',l'}$, i.e.,

$$\check{H}^{m,p}_{n',l'} = \frac{R^{m,p}_{n',l'}}{S^{m}_{n',l'}} = H^{m,p}_{n',l'} + \frac{Z^{p}_{n',l'}}{S^{m}_{n',l'}}, \quad \forall \{n',l'\} \in \mathcal{P}^m, \tag{1}$$

where $Z^{p}_{n',l'}$ denotes the additive white Gaussian noise component at the pth receive antenn and $\mathcal{P}^m$ denotes the set of pilot symbol positions in the OFDM frame from the mth transmit antenna. Note that the division by $S^{m}_{n',l'}$ in (1) can be replaced with a multiplication of the conjugate complex value $(S^{m}_{n',l'})^*$ if the pilot symbols are taken from a phase shift keying (PSK) symbol alphabet with unit energy. Otherwise, the initial estimates can be only obtained through (1).

2) The final estimates of the complete channel transfer function belonging to the desired OFDM frame are obtained from the initial estimates $\check{H}^{m,p}_{n',l'}$ by two-dimensional (2-D) filtering. The 2-D filtering is given by

$$\hat{H}^{m,p}_{n,l} = \sum_{\{n',l'\} \in \mathcal{T}^m_{n,l}} \omega^{m}_{n',l',n,l}\, \check{H}^{m,p}_{n',l'} \qquad \mathcal{T}^m_{n,l} \in \mathcal{P}^m,\ n = 1,\ldots,N_{\mathrm{c}},\ l = 1,\ldots,N_{\mathrm{s}}, \tag{2}$$

where $\omega^{m}_{n',l',n,l}$ is the shift-variant 2-D impulse response of the filter. The subset $\mathcal{T}^m_{n,l} \in \mathcal{P}^m$ is the set of initial estimates $\check{H}^{m,p}_{n',l'}$ that are used for estimation of $\hat{H}^{m,p}_{n,l}$. The number of filter coefficients is

$$N^m_{\mathrm{tap}} = ||\mathcal{T}^m_{n,l}|| \leq N^m_{\mathrm{grid}} = ||\mathcal{P}^m||. \tag{3}$$

The optimum solution to the filtering problem of (2) in the MSE sense is the 2-D Wiener filter [5], i.e.,

$$\boldsymbol{\omega}_{n,l}^{m} = \left(\boldsymbol{\phi}^{m}\right)^{-1} \boldsymbol{\theta}_{n,l}^{m}. \tag{4}$$

The vector elements of the crosscorrelation $\boldsymbol{\theta}_{n,l}^{m}$ and the matrix elements of the autocorrelation $\boldsymbol{\phi}^{m}$ are

$$\theta_{n-n'',l-l''}^{m} = \mathrm{E}\left\{ H_{n,l}^{m,p} \left(H_{n'',l''}^{m,p} \right)^{*} \right\} \quad \forall \{n'', l''\} \in \mathcal{T}_{n,l}^{m}, \tag{5}$$

The expectation in (5) is only non-zero for the same pair of transmit and receive antennas $\{m, p\}$ due to the i.i.d. subchannels. Therefore, $\theta_{n-n'',l-l''}^{m}$ only depends on the transmit antenna index m because the set of pilot positions $\mathcal{T}_{n,l}^{m}$ differs from each transmit antenna. For notational convenience, we drop the index m for the crosscorrelation in the following. The matrix elements of the autocorrelation $\boldsymbol{\phi}^{m}$ are

$$\phi_{n'-n'',l'-l''}^{m} = \theta_{n'-n'',l'-l''}^{m} \quad + \mathrm{E}\left\{ \frac{1}{|S_{n',l'}^{m}|^{2}} \right\} \sigma^{2}\, \delta_{n'-n'',l'-l''}, \forall \{n', l'\}, \{n'', l''\} \in \mathcal{T}_{n,l}^{m}, \tag{6}$$

with σ^2, $\mathrm{E}\{\frac{1}{|S_{n',l'}^{m}|^{2}}\}$, $\delta_{n'-n'',l'-l''}$ being the average noise variance, the mean pilot symbol energy, and the Kronecker delta function. $\{n'', l''\}$ denotes only pilot symbol positions. According to (5), the autocorrelation depends only on the distances between the pilot positions and, hence, it is independent of the actual CE position $\{n, l\}$.

Due to the WSSUS assumption of the channel [6], the correlation function $\theta_{n-n'',l-l''}$ can be separated into two independent parts

$$\theta_{n-n'',l-l''} = \theta_{n-n''} \cdot \theta_{l-l''}, \quad \forall \{n'', l''\} \in \mathcal{T}_{n,l}^{m} \tag{7}$$

with $\theta_{n-n''}$ and $\theta_{l-l''}$ representing the discrete frequency and time correlation functions. This allows to replace the 2-D filter by two cascaded 1-D filters, one for filtering in frequency direction and the other one for filtering in time direction.

Since in practice the correlation function $\theta_{n-n'',l-l''}$ is unknown at the receiver, the channel estimation filters have to be designed robust so that they cover a great variety of delay and Doppler PSDs. According to [5], a uniform delay PSD ranging from 0 to τ_{filter} and a uniform Doppler PSD ranging from $-f_{D_{\mathrm{filter}}}$ to $f_{D_{\mathrm{filter}}}$ fulfill the robust design requirements. Thus, the discrete frequency correlation function results in

$$\theta_{n-n''} = \frac{\sin(\pi \tau_{\mathrm{filter}}(n-n'')\Delta f)}{\pi \tau_{\mathrm{filter}}(n-n'')\Delta f} e^{-j\pi\tau_{\mathrm{filter}}(n-n'')\Delta f}, \quad \forall n'' \in \mathcal{T}_{n,l}^{m} \tag{8}$$

and the discrete time correlation function yields

$$\theta_{l-l''} = \frac{\sin(2\pi f_{D_{\mathrm{filter}}}(l-l'')T_{\mathrm{s}}')}{2\pi f_{D_{\mathrm{filter}}}(l-l'')T_{\mathrm{s}}'}, \quad \forall l'' \in \mathcal{T}_{n,l}^{m} \tag{9}$$

where Δf denotes the subcarrier spacing, T_{s}' the duration of one OFDM symbol including the guard interval T_{GI}.

Moreover, the signal-to-noise ratio (SNR) in (6) can be set to a predetermined value [5]. Thus, robust PACE only requires knowledge of the maximum channel delay τ_{filter}, the maximum Doppler frequency $f_{D_{\mathrm{filter}}}$, and a predetermined SNR value. With such a robust design, a set of filter coefficients can be precomputed to reduce the complexity of the channel estimation.

However, due to the model mismatch in the correlation function $\theta_{n-n'',l-l''}$, the robust Wiener filter performs significantly worse for certain channel models than a perfect channel estimation. Therefore, we apply ICE to improve the CSI estimate.

B. Least-squares estimation in iterative channel estimation

In the following the LS estimate in (1) is investigated in detail for ICE. Here, we consider an MC-CDMA system with Walsh-Hadamard spreading codes. [13] demonstrates that due to the superposition of Walsh-Hadamard spread data signals (chips), zero-valued subcarriers can occur in the transmit signal. For instance, Fig. 3 shows the possible constellation points and their relative occurrence for a binary phase shift keying (PSK) symbol alphabet and a spreading length of 8. As inferred, a zero-valued subcarrier occurs with 27% probability. In the case of 4-QAM, symbol alphabet and spreading length of 8, the probability of a zero-valued subcarrier is reduced to 8%, but it is still significant. In addition, small amplitudes can occur on subcarriers causing noise enhancement in the LS estimates. Consequently, a method must be found for avoiding a division by zero and noise enhancement in the LS estimation of (1).

Several researchers [7]–[11] have investigated ICE for spread spectrum and multi-carrier systems. Yet, they do not consider ICE employing the two step CE described by (1) and (2) for downlink MIMO MC-CDMA and Walsh-Hadamard spreading [12]. Thus, the above problem of a division by zero in the LS estimation is not addressed.

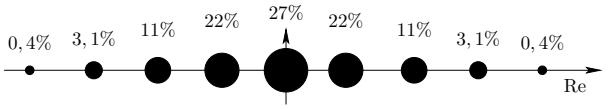

Fig. 3. Constellation points of a subcarrier with binary PSK symbol alphabet and spreading length 8

Therefore, we propose the following MIMO MLS channel estimation method: If the magnitude of the reconstructed subcarrier is zero, equal to, or below the threshold $\rho_{\mathrm{th}} \geq 0 \in \mathbb{R}$, the initial estimate $\check{H}_{n,l}^{(i),m,p}$ is set to zero, i.e.,

$$\check{H}_{n,l}^{(i),m,p} = \begin{cases} \frac{R_{n,l}^{(i),m,p}}{\check{S}_{n,l}^{(i),m}} & : \{n,l\} \in \bar{\mathcal{D}} \text{ and } |\check{S}_{n,l}^{(i),m}| > \rho_{\mathrm{th}}, \\ 0 & : \{n,l\} \in \bar{\mathcal{D}} \text{ and } |\check{S}_{n,l}^{(i),m}| \leq \rho_{\mathrm{th}}, \end{cases} \tag{10}$$

where $\check{S}_{n,l}^{(i),m}$ denotes an estimated data symbol in the ith iteration of ICE and $R_{n,l}^{(i),m,p}$ is the received signal only comprised of the mth transmit signal $S_{n,l}^{m}$. In Section III-C, we explain how to obtain $R_{n,l}^{(i),m,p}$. The threshold ρ_{th} should be chosen so that noise enhancement caused by subcarriers with small or zero-valued amplitudes is avoided and only a few possible constellation points of a subcarrier are below the threshold. Choosing ρ_{th} too large will reduce the performance gain of ICE compared to PACE for medium to high SNRs as only few subcarriers in addition to the pilot symbols will be used in ICE. In contrast, choosing ρ_{th} too small will degrade the performance of ICE only for low SNRs. Hence, the initial estimates in (10) will not cause noise enhancement and degrade the channel estimates. Furthermore, both soft- and hard-decided symbols can be used for ICE. Note, if the data symbols are taken from a PSK symbol alphabet before spreading and the spreading length is greater than one, it is not possible to replace the division in (10) by a multiplication with $\left(\check{S}_{n',l'}^{(i),m}\right)^{*}$.

C. Extension of iterative channel estimation to MIMO MC-CDMA system

Since the pilot symbols for different transmit antennas are transmitted on disjoint positions and assuming i.i.d. subchannels, PACE for an MIMO MC-CDMA system is a straight forward extension of PACE for a SISO MC-CDMA system. In ICE, however, the data symbols from different transmit antennas are not placed on disjoint positions or generally orthogonal, which results in the following superposition

$$R_{n,l}^{p} = \sum_{r=1}^{N_{\mathrm{TX}}} H_{n,l}^{r,p}\, S_{n,l}^{r}, \qquad \{n,l\} \in \bar{\mathcal{D}}. \tag{11}$$

Hence, (10) cannot be directly applied when using previously decided data symbols $\check{S}_{n,l}^{(i),m}$.

To obtain an interference reduced received signal $R_{n,l}^{(i),m,p}$ for (10), we subtract the estimated transmit signals except for the mth antenna, i.e.,

$$R_{n,l}^{(i),m,p} = R_{n,l}^{p} - \sum_{\substack{r=1 \\ r \neq m}}^{N_{\mathrm{TX}}} \hat{H}_{n,l}^{(i-1),r,p} \check{S}_{n,l}^{(i),r}, \;\; \{n,l\} \in \bar{\mathcal{D}}. \tag{12}$$

Thus, we initially estimate the CSI between transmit antenna m and receive antenna p by first canceling the current estimates of the received signals from the other transmit antennas and subsequently applying (10).

D. Iterative channel estimation (ICE)

As explained in Section II, the initially estimated CSI in (2) is then used in the MUD/SUD block and decoder to obtain an initial estimate of the transmitted information bits. After reconstructing the transmitted signal from the estimated information bits (Section II), the estimated data symbols and the transmitted pilot symbols form the set $\mathcal{P}_{\mathrm{ICE}}^{m} = \mathcal{P}^{m} \cup \bar{\mathcal{D}}$ of reference symbols known at the receiver. The set $\mathcal{P}_{\mathrm{ICE}}^{m}$ defines the complete frame of pilot and data symbols from transmit antenna m.

For ICE with one or more iterations ($i > 0$), the following steps have to be executed in each iteration:

1) Reconstruct the transmit signal $\check{S}_{n,l}^{(i),m}\ \forall \{n,l\} \in \bar{\mathcal{D}}$ and $m = 1, \ldots, N_{\mathrm{TX}}$ from the estimate of the transmitted information bits.
2) Compute the interference reduced received signal $R_{n,l}^{(i),m,p}$ for transmit antenna m and receive antenna p in (12).
3) Calculate the initial estimates $\check{H}_{n,l}^{(i),m,p}$ for reference symbols in $\bar{\mathcal{D}}$ according to (10).
4) Obtain the final estimate of the channel transfer function between transmit antenna m and receive antenna p through filtering the initial estimates over the set $\mathcal{P}_{\mathrm{ICE}}^{m}$ of all reference symbols, i.e.,

$$\hat{H}_{n,l}^{(i),m,p} = \sum_{\{n',l'\} \in \mathcal{T}_{n,l}^{m}} \omega_{n',l',n,l}^{(i),m}\, \check{H}_{n',l'}^{(i),m,p} \qquad \mathcal{T}_{n,l}^{m} \subseteq \mathcal{P}_{\mathrm{ICE}}^{m}, \;\; n = 1, \ldots, N_{\mathrm{c}},\, l = 1, \ldots, N_{\mathrm{s}}, \tag{13}$$

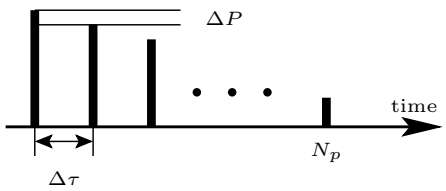

Fig. 4. Power delay profile of the simulated channel model

TABLE I
SYSTEM PARAMETERS

Parameter	Characteristic/Value
Carrier frequency	5 GHz
Bandwidth	101.25 MHz
Subcarriers	768
FFT length	1024
Sampling duration T_{spl}	7.4 ns
Guard interval T_{GI}	$226\,T_{\mathrm{spl}}$
Subcarrier spacing Δf	131.836 kHz
OFDM symbols / frame	64
Spreading factor	8
Users	1, 8
M parallel data symbols	96
Data modulation	QPSK, Gray mapping
Coding type	conv. code $R = 1/2$ $(133, 171)$
Detection technique	MMSE, soft PIC
Interleaver	Random Frequency
Transmit antennas	1, 2
Receive antennas	1
Space-time code	none, Alamouti
Pilot distance frequency N_{l}	3
Pilot distance time N_{k}	9

where $\omega_{n',l',n,l}^{(i),m}$ is the Wiener filter coefficient obtained for the ith iteration. Note, contrary to previous notation, $\{n', l'\}$ here denotes both pilot and data symbols.

5) Use the newly estimated CSI $\hat{H}_{n,l}^{(i),m,p}$ from (13) in the subsequent MUD/SUD block and decoder to obtain a new estimate of the transmitted information bits.

Similar to Section III-A, the Wiener filters in the 4th step can be designed robust with respect to the channel statistics. Hence, merely a second set of filter coefficients need to be precomputed keeping the complexity of the CE in Fig. 1(a) low within ICE.

IV. SIMULATION RESULTS

This section presents simulation results for a downlink MIMO MC-CDMA system applying Walsh-Hadamard spreading and the Alamouti STBC [4] with perfect CE, PACE, and ICE. The simulation parameters are listed in Table I and the power delay profile of the channel model is depicted in Fig. 4. The non-zero tap spacing of the power delay profile $\Delta\tau$ is 16 samples and the maximum delay $\tau_{\max}$ is 176 samples. The channel employs $N_{\mathrm{p}} = 12$ taps with a power decrement ΔP of 1 dB. The Doppler frequencies are distributed according to a Jakes' spectrum and the maximum Doppler frequency $f_{D_{\max}}$ is 1500 Hz ($\approx 0.01\ \Delta f$), which is related to a mobile terminal speed of 300 km/h at $f_{\mathrm{c}} = 5$ GHz.

For robust PACE and ICE, two 1-D Wiener filters are cascaded with 15 filter coefficients in frequency direction and 4 in time direction to compute the CSI estimates in (2). The delay and Doppler PSDs are uniformly distributed with a maximum delay $\tau_{\mathrm{filter}} = T_{\mathrm{GI}}$ and a maximum Doppler frequency $f_{\mathrm{D_{filter}}} = 1500$ Hz. In the case of perfect CE, no pilot symbols are transmitted. Thus, the SNR loss for transmitting pilot symbols for PACE or ICE is 0.185 dB.

The simulation results in Figs. 5 and 6 demonstrate that the proposed ICE can improve PACE. Since ICE requires the detection of all the signals from all the users, the MMSE SUDs are applied to all K user signals. For ICE and the parallel interference canceler (PIC) MUD one iteration is computed. Simulation results indicate that additional iterations only yield little improvements and hence, are omitted for clarity.

The MSE versus E_{b}/N_0 is plotted in Fig. 5. For SNRs below 2 dB, robust PACE outperforms robust ICE as decoding errors lead to wrong CSI estimates in (10). For SNRs above 2 dB, robust ICE can outperform robust PACE. The influence of the threshold on the MSE for the MLS method is significant. Setting $\rho_{\mathrm{th}} = 0.8$ results in an MSE of 0.24 at $E_{\mathrm{b}}/N_0 = 10$ dB as

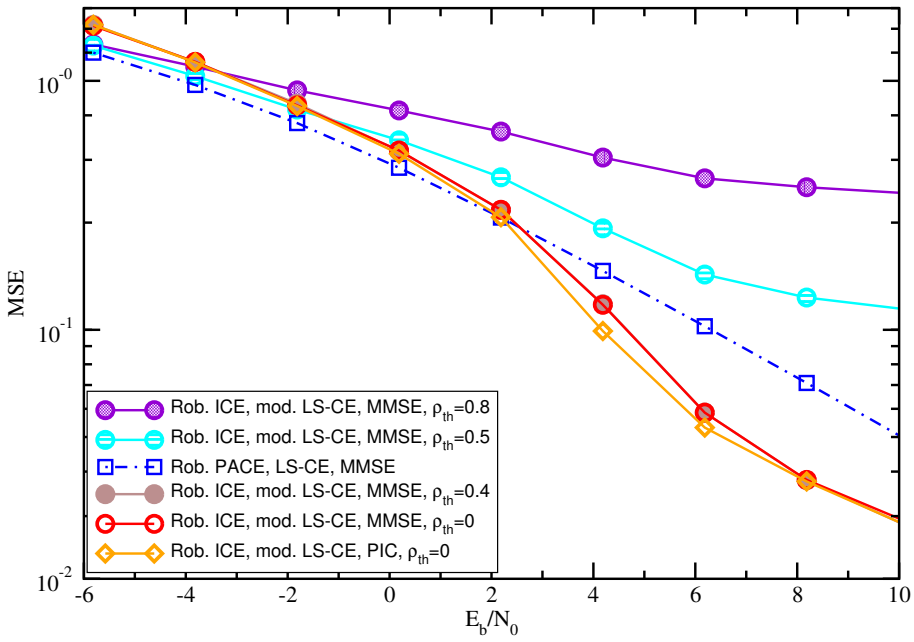

Fig. 5. MMSE comparison of robust PACE and robust ICE for MMSE SUD, PIC MUD, and fully-loaded system

ICE does not use 50% of the possible constellation points. The MSE is reduced to 0.11 when decreasing ρ_{th} to 0.5 neglecting 30% of the constellation points. For $\rho_{\mathrm{th}} < 0.5$, only zero-valued subcarriers are ignored in ICE (8% of the constellation points). Thus, the curves for $\rho_{\mathrm{th}} = 0.4$ and $\rho_{\mathrm{th}} = 0$ coincide. Further, noise enhancement resulting from small thresholds for low SNRs has little influence on the MSE performance compared to decoding errors in ICE.

Fig. 6 displays simulated BER curves for the different CE methods. The threshold ρ_{th} is set to zero to avoid a division by zero and noise enhancement by zero-valued subcarriers. Thus, the maximum number of useful constellation points is exploited in ICE. Note that the pilot spacing and the robust PACE are optimized for this channel model. Hence, the results for the proposed ICE in Fig. 6(a) are very promising since it still gains about 0.8 dB and 0.9 dB for the MMSE SUD and the PIC MUD compared to PACE with the corresponding detectors at a BER of 10^{-4}. The performance loss of ICE compared to perfect CE is reduced to 1 dB for the MMSE SUD and the PIC MUD at a BER of 10^{-4}.

In Fig. 6(b), the Alamouti scheme is applied in time direction over two consecutive OFDM symbols. For a maximum te coherence time of the channel is about 120 μs whereas the duration of one OFDM symbol is only about 9.5 μs. So, the channel is approximately constant over two consecutive OFDM symbols, which is a necessary prerequisite for the Alamouti scheme. For this channel model, the Alamouti scheme improves the performance of the SISO MC-CDMA system by 0.8 dB, 1.5 dB and 2.1 dB for the SUB, PIC, and MMSE SUD with perfect CE at a BER of 10^{-4}. In the MIMO system all pilot distances for different transmit antennas are the same as in the SISO system. So, in total, the MIMO system employs twice as much pilots as the SISO system. To keep the total transmitted pilot symbol energy constant, the pilot symbol energy for each transmit antenna is scaled by $1/N_{\mathrm{TX}}$ allowing a fair comparison between the SISO and MIMO channel estimation. This explains, why the performance gains for PACE and ICE are only 0.8 dB for the MMSE SUD, 0.3 dB for PACE and PIC MUD, and 0 dB for ICE and PIC MUD at a BER of 10^{-4} . When applying the Alamouti STBC in Fig. 6(b), ICE performs about 0.6 dB better than PACE for both MMSE SUD and PIC MUD at a BER of 10^{-4}.

V. CONCLUSIONS

In this paper, we present a downlink MC-CDMA system with Walsh-Hadamard spreading codes applying ICE at the receiver. Since the superposition of Walsh-Hadamard spread data signals (chips) can result in zero-valued subcarriers, the LS channel estimates within ICE cannot be computed. Further, the transmitted data signals coincide non-orthogonal at each receive antenna. Thus, we propose the modified LS MIMO channel estimation method to resolve these problems and avoid noise enhancement. Simulation results indicate that the MC-CDMA receiver with robust ICE and the modified LS method can outperform robust PACE by roughly 1 dB even for scenarios that were optimized for robust PACE.

Moreover, the modified LS channel estimation can be applied with ICE to any other MC-CDMA, multi-carrier, CDMA, or spread spectrum system with general spreading codes or symbol alphabet whose superposition or constellation yields values below a certain threshold.

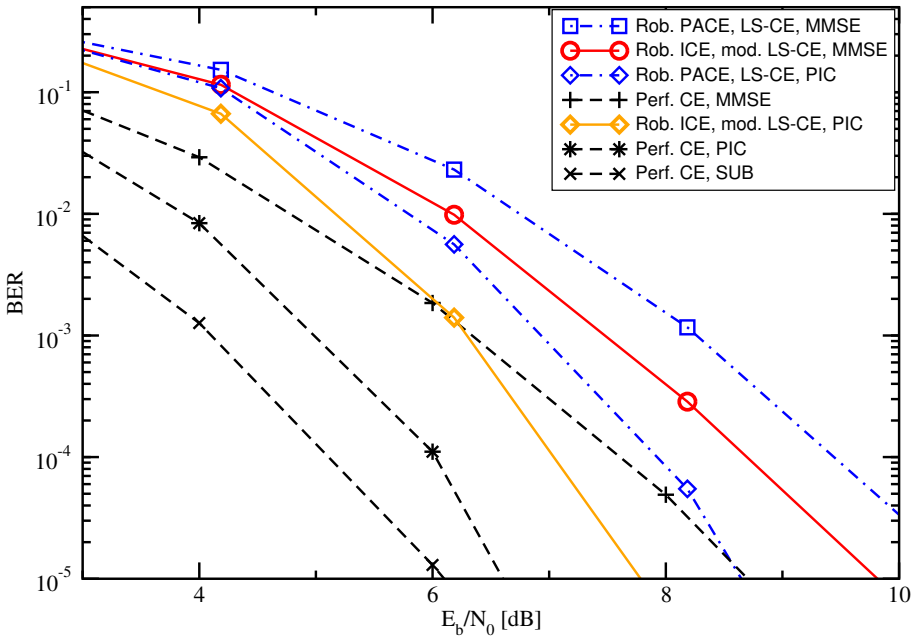

(a) SISO

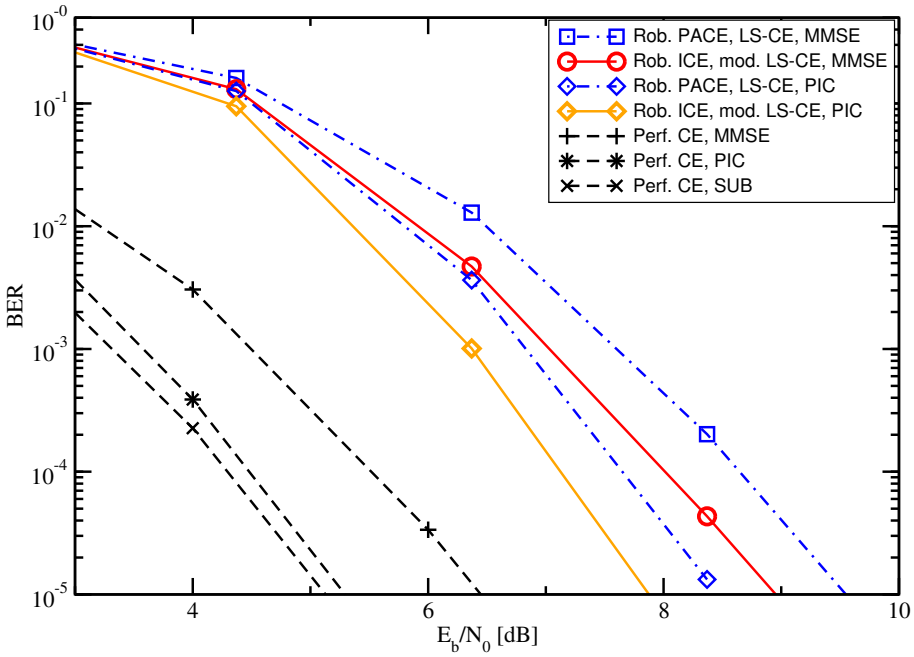

(b) Alamouti STBC

Fig. 6. Comparison of perfect, robust PACE, and robust ICE for MMSE SUD, PIC MUD, and fully-loaded system for (a) SISO MC-CDMA system and (b) MC-CDMA system employing Alamouti STBC

ACKNOWLEDGMENT

The work presented in this paper was supported by the European IST projects 4MORE (4G MC-CDMA multiple antenna system On chip for Radio Enhancements) and WINNER (Wireless World Initiative New Radio) [http://ist-4more.org/ and http://ist-winner.org].

REFERENCES

[1] J. Bingham, "Multicarrier modulation for data transmission: An idea whose time has come," *IEEE Commun. Mag.*, vol. 28, pp. 5–14, May 1991.
[2] K. Fazel and L. Papke, "On the performance of convolutionally-coded CDMA/OFDM for mobile communication systems," in *Proc. of IEEE PIMRC'93*, Yokohama, Japan, Sep. 1993, pp. 468–472.
[3] Y. Kishiyama, *et al.*, "Experiments on throughput performance above 100-Mbps in forward link for VSF-OFDCDM broadband packet wireless access," in *Proc. of IEEE VTC'F03*, Orlando, USA, Oct. 2003, pp. 1863–1868.
[4] S. M. Alamouti, "A simple transmit diversity technique for wireless communications," *IEEE Journal on Selected Areas in Communications*, vol. 16, no. 8, pp. 1451–1458, October 1998.
[5] K. Fazel and S. Kaiser, *Multi-Carrier and Spread Spectrum Systems*. John Wiley and Sons, 2003.
[6] P. Hoeher, "A statistical discrete-time model for the WSSUS multipath channel," *IEEE Trans. Veh. Technol.*, vol. 41, no. 4, pp. 461–468, Nov. 1992.
[7] V. Mignone and A. Morello, "CD3-OFDM: A novel demodulation scheme for fixed and mobile receivers," *IEEE Trans. Commun.*, pp. 1144–1151, Sept. 1996.
[8] P. Frenger and A. Svensson, "Decision directed coherent detection in multicarrier systems on Rayleigh fading channels," *IEEE Trans. Veh. Technol.*, pp. 490–498, Mar. 1996.
[9] D. Kalofonos, M. Stojanovic, and J. Proakis, "Performance of adaptive MC-CDMA detectors in rapidly fading rayleigh channels," *IEEE Trans. Wireless Commun.*, pp. 229–239, Mar. 2003.
[10] T. Zemen, *et al.*, "Improved channel estimation for iterative receivers," in *Proc. of IEEE GLOBECOM'03*, San Francisco, USA, Dec. 2003.
[11] F. Sanzi, S. Jelting, and J. Speidel, "A comparative study of iterative channel estimators for mobile OFDM systems," *IEEE Trans. Wireless Commun.*, pp. 849–859, Sept. 2003.
[12] S. Sand, R. Raulefs, and G. Auer, "Iterative channel estimation for high mobility broadband MC-CDMA systems," in *Proc. IEEE ICC'05*, Seoul, Korea, May 2005.
[13] A. Bury, J. Egle, and J. Lindner, "Diversity comparison of spreading transforms for multicarrier spread spectrum transmission," *IEEE Trans. Commun.*, vol. 51, no. 5, pp. 774–781, May 2003.